Sauter-Schwinger Effect for Colliding Laser Pulses

Christian Kohlfürst,[1] Naser Ahmadiniaz,[1] Johannes Oertel,[2] and Ralf Schützhold[1,3]
[1]*Helmholtz-Zentrum Dresden-Rossendorf, Bautzner Landstraße 400, 01328 Dresden, Germany*
[2]*Fakultät für Physik, Universität Duisburg-Essen, Lotharstraße 1, 47057 Duisburg, Germany*
[3]*Institut für Theoretische Physik, Technische Universität Dresden, 01062 Dresden, Germany*

(Received 17 December 2021; accepted 27 October 2022; published 5 December 2022)

Via a combination of analytical and numerical methods, we study electron-positron pair creation by the electromagnetic field $\boldsymbol{A}(t,\boldsymbol{r}) = [f(ct-x)+f(ct+x)]\boldsymbol{e}_y$ of two colliding laser pulses. Employing a generalized Wentzel-Kramers-Brillouin approach, we find that the pair creation rate along the symmetry plane $x=0$ (where one would expect the maximum contribution) displays the same exponential dependence as for a purely time-dependent electric field $\boldsymbol{A}(t) = 2f(ct)\boldsymbol{e}_y$. The prefactor in front of this exponential does also contain corrections due to focusing or defocusing effects induced by the spatially inhomogeneous magnetic field. We compare our analytical results to numerical simulations using the Dirac-Heisenberg-Wigner method and find good agreement.

DOI: 10.1103/PhysRevLett.129.241801

Introduction.—As one of the most striking and fundamental predictions of quantum electrodynamics (QED), the vacuum should become unstable in the presence of strong electric fields, leading to the spontaneous creation of electron-positron pairs (“matter from light”) [1,2]. For a constant electric field E, the pair-creation probability P displays an exponential dependence ($\hbar = c = 1$)

$$P \sim \exp\left\{-\pi\frac{m^2}{qE}\right\} = \exp\left\{-\pi\frac{E_S}{E}\right\}, \tag{1}$$

with the electron mass m and elementary charge q, which can be combined to yield the Schwinger critical field $E_S = m^2/q \approx 1.3\times 10^{18}$ V/m. The above functional dependence does not admit a Taylor expansion in q which indicates that this Sauter-Schwinger effect (1) is a nonperturbative phenomenon [3,4]. As a result, the corresponding calculations can be quite nontrivial and our knowledge beyond the case of constant fields is very limited [5,6]. For slowly varying fields, we may apply the locally constant field approximation by evaluating Eq. (1), together with its generalization to additional magnetic fields, at each spacetime point [7,8]. However, this approximation has a limited range of applicability and does not capture many important effects, such as the dynamically assisted Sauter-Schwinger effect [9–12].

From a fundamental point of view as well as in anticipation of experimental initiatives aiming at ultrahigh field strengths [13], it is important to better understand the Sauter-Schwinger effect for nonconstant fields [14,15]. While there has been progress regarding fields which depend on one coordinate (e.g., space x or time t [16,17], or a light-cone variable $t-x$ [18,19]), our understanding of more complex field dependences, e.g., the interplay between spatial and temporal variations, is still in its infancy [20,21]. Furthermore, going from simple models toward realistic field configurations requires the consideration of transversal fields which are vacuum solutions of the Maxwell equations. In the following, we venture a step into this direction by employing a combination of analytical and numerical methods.

The model.—In order to treat a potentially realistic yet simple field configuration, we consider the head-on collision of two equal plane-wave laser pulses, see also Ref. [22]

$$\boldsymbol{A}(t,\boldsymbol{r}) = [f(t-x)+f(t+x)]\boldsymbol{e}_y. \tag{2}$$

For asymmetric collision scenarios, see, e.g., [23–27]. This vector potential (2) is an even function of x, i.e., $A_y(t,x) = A_y(t,-x)$ such that $\partial_x A_y(t,x=0) = 0$. Thus, along the symmetry plane $x=0$, the electric field components E_y add up while the magnetic fields B_z of the two pulses cancel each other. As a result, one would expect the maximum contribution to pair creation there.

In the following, we assume that the typical frequency scale ω describing the rate of change of the function $f(t)$ is subcritical, i.e., much smaller than the electron mass $\omega \ll m$. The characteristic electric field strength E should also be subcritical $E \ll E_S$ and the Keldysh parameter (or inverse laser parameter $1/a_0$) [28–31]

$$\gamma = \frac{m\omega}{qE} = \frac{1}{a_0}, \tag{3}$$

should be roughly of order unity such that $qE = \mathcal{O}(\omega m)$.

WKB approach.—In this limit, where the electron mass m is the largest scale, we may employ semiclassical methods such as world-line instantons [20,32–34] discussed in Sec. A of Supplemental Material [35] or the Wentzel-Kramers-Brillouin (WKB) approach [51,52] used here. For simplicity and because spin effects are not expected to play a major role here, we start from the Klein-Fock-Gordon equation

$$[(\partial_\mu + iqA_\mu)(\partial^\mu + iqA^\mu) - m^2]\phi = 0. \tag{4}$$

Via the standard WKB ansatz [53]

$$\phi(t,x,y,z) = \alpha(t,x)e^{iS(t,x,y,z)}, \tag{5}$$

we split ϕ into a slowly varying amplitude α and a rapidly oscillating phase e^{iS}. More precisely, $\partial_\mu S$ and qA_μ are large quantities of the order of the electron mass $\mathcal{O}(m)$ while $\partial_\mu \alpha = \mathcal{O}(\omega)$ is much smaller. Inserting this ansatz (5) into Eq. (4), the leading order $\mathcal{O}(m^2)$ yields the eikonal equation $(\partial_\mu S + qA_\mu)(\partial^\mu S + qA^\mu) = m^2$. In view of the translational invariance in y and z, we make the separation ansatz $S(t,x,y,z) = k_y y + k_z z \pm s(t,x)$, where $s(t,x)$ is determined by the first-order equation

$$\partial_t s = \sqrt{m^2 + (\partial_x s)^2 + (k_y + qA_y)^2 + k_z^2}. \tag{6}$$

We expect the maximum contribution to pair creation along the symmetry plane $x = 0$ where the electric field assumes its maximum, i.e., from those wave packets staying close to $x = 0$ throughout the evolution, which implies zero momentum in the x direction $\partial_x s|_{x=0} = 0$ [54]. Thus (and since A_y is an even function of x), we take $s(t,x)$ to be an even function of x for simplicity. After a Taylor expansion around $x = 0$

$$s(t,x) = s_0(t) + \frac{x^2}{2} s_2(t) + \mathcal{O}(x^4), \tag{7}$$

we find that the zeroth order $s_0(t)$, i.e., the eikonal along $x = 0$ is given by

$$\partial_t s_0 = \sqrt{m^2 + [k_y + qA_y(t, x = 0)]^2 + k_z^2}, \tag{8}$$

in complete analogy to a purely time-dependent field.

Focusing and defocusing effects.—As the next step, let us study the impact of the curvature $s_2(t)$ in Eq. (7). Having determined the phase function S by the leading-order $\mathcal{O}(m^2)$ contribution to Eq. (4), the subleading order $\mathcal{O}(m\omega)$ determines the evolution of α via

$$(\partial^\mu s)\partial_\mu \alpha = -\frac{\alpha}{2}\Box s, \tag{9}$$

where the higher-order term $\Box\alpha = \mathcal{O}(\omega^2)$ has been neglected. Along the symmetry plane $x = 0$ where $\partial_x s = 0$, the spatial derivative $\partial_x \alpha$ drops out and thus the left-hand side of Eq. (9) is again the same as in a purely time-dependent field.

The right-hand side of Eq. (9), on the other hand, contains the additional term $\partial_x^2 s|_{x=0} = s_2$. This curvature contribution can be obtained by inserting Eq. (7) into Eq. (6) followed by a Taylor expansion

$$\partial_t s_2 = \left. \frac{s_2^2 + [k_y + qA_y]q\partial_x^2 A_y}{\sqrt{m^2 + [k_y + qA_y]^2 + k_z^2}} \right|_{x=0}. \tag{10}$$

In analogy to Eq. (8), we obtain a closed ordinary differential equation for $s_2(t)$. In contrast to Eq. (8), however, this is a nonlinear equation which can display (blowup) singularities. Similar to caustics, they do not imply singularities of the solutions ϕ to the original (linear) Klein-Fock-Gordon equation (4), but indicate a breakdown of the WKB ansatz (5), as also discussed in [55]. Fortunately, for a large class of parameters including the cases of interest here, such singularities do not occur—see also Sec. F in Supplemental Material [35].

In order to provide an intuitive interpretation of the above equation (10), we note that $k_y + qA_y$ is the mechanical momentum in the y direction, proportional to the velocity v_y. As $\partial_x A_y$ is the magnetic field B_z, the numerator in Eq. (10) yields, apart from the nonlinearity s_2^2, the divergence $\partial_x F_x$ of the Lorentz force. Thus, the curvature s_2 is associated with the focusing or defocusing effect of the inhomogeneous magnetic field B_z.

Particle creation.—The simple WKB ansatz (5) is not well suited for studying pair creation because this phenomenon is associated with a mixing of positive and negative frequency solutions, which is not captured by the ansatz (5) for slowly varying α. Thus, we adapt a generalized WKB ansatz, see also Refs. [55–57].

To this end, we define the phase-space pseudovector $\boldsymbol{\varphi} = (\phi, \dot{\phi})^T$ which allows us to cast the original second-order equation (4) into a first-order form

$$\partial_t \boldsymbol{\varphi} = \begin{pmatrix} 0 & 1 \\ \partial_x^2 - \mu^2 & 0 \end{pmatrix} \cdot \boldsymbol{\varphi} = [\boldsymbol{\sigma}_+ + \boldsymbol{\sigma}_-(\partial_x^2 - \mu^2)] \cdot \boldsymbol{\varphi}, \tag{11}$$

where $\boldsymbol{\sigma}_\pm$ are the Pauli ladder matrices and $\mu(t,x)$ denotes the effective mass $\mu^2 = m^2 + (k_y + qA_y)^2 + k_z^2$.

In order to include pair creation, we generalize the original WKB ansatz (5) via

$$\boldsymbol{\varphi} = \alpha \boldsymbol{u}_+ e^{+is} + \beta \boldsymbol{u}_- e^{-is}, \tag{12}$$

where $\alpha(t,x)$ and $\beta(t,x)$ are the Bogoliubov coefficients, which are assumed to be slowly varying. The basis vectors $\boldsymbol{u}_\pm(t,x)$ are eigenvectors of the matrix

$$[\boldsymbol{\sigma}_+ - \boldsymbol{\sigma}_-([\partial_x s]^2 + \mu^2)] \cdot \boldsymbol{u}_\pm = \pm i\chi \boldsymbol{u}_\pm, \tag{13}$$

with eigenvalues $\pm i\chi$ where $\chi(t,x) = \partial_t s(t,x)$ is given by Eq. (6). Thus, after inserting the generalized ansatz (12) into Eq. (11), the leading order again corresponds to the eikonal equation (6).

For simplicity, we use the (non-normalized) eigenvectors $\boldsymbol{u}_\pm = (1, \pm i\chi)^T$ in the following. Since A_y and s are even functions of x, the first x derivatives of s, μ, χ, and $\boldsymbol{u}_\pm$, vanish along the symmetry plane $x = 0$. Furthermore, although the second x derivatives of μ, χ, $\boldsymbol{u}_\pm$, α, and β do not vanish along the symmetry plane $x = 0$, they scale with $\mathcal{O}(\omega^2)$. Thus, they are neglected within the next-to-leading order $\mathcal{O}(m\omega)$ of the WKB approach, which yields (along the symmetry plane $x = 0$)

$$\begin{aligned}(\dot{\alpha}\boldsymbol{u}_+ + \alpha\dot{\boldsymbol{u}}_+ - i\alpha\boldsymbol{\sigma}_- \cdot \boldsymbol{u}_+ \partial_x^2 s)e^{+is} \\ + (\dot{\beta}\boldsymbol{u}_- + \beta\dot{\boldsymbol{u}}_- + \beta\boldsymbol{\sigma}_- \cdot \boldsymbol{u}_- \partial_x^2 s)e^{-is} = 0.\end{aligned} \tag{14}$$

Note that $\partial_x^2 s = \mathcal{O}(m\omega)$ is kept, in complete analogy to Eq. (9). Projection with $\boldsymbol{u}_\pm^\perp = (\pm i\chi, 1)^T$ gives

$$\begin{aligned}2\chi\dot{\alpha} + \alpha\Box s &= \beta(\Box s)e^{-2is}, \\ 2\chi\dot{\beta} + \beta\Box s &= \alpha(\Box s)e^{+2is}.\end{aligned} \tag{15}$$

For the spatially homogeneous limit where $\partial_x^2 s = 0$, we recover the well-known evolution equations for a purely time-dependent field as $\Box s \to \ddot{s}$. For our colliding-pulse scenario (2), these two evolution equations (15) for α and β along the $x = 0$ plane contain the same exponents $e^{\pm is}$ as in the case of a purely time-dependent field, the only difference are the prefactors $\Box s$ which now contain the additional $\partial_x^2 s$ term. The $\ddot{s}$ contribution $\partial_t^2 s = \partial_t \chi = q\dot{A}_y(k_y + qA_y)/\chi$ already present in a purely time-dependent scenario contains the electric field E_y while the additional $\partial_x^2 s$ contribution stems from the inhomogeneities of the magnetic field B_z and describes the focusing or defocusing effects discussed below.

As in the purely time-dependent scenario, we may combine the two linear evolution equations (15) for the Bogoliubov coefficients into a single Riccati equation $\dot{R} = \Box s(e^{+2is} - R^2 e^{-2is})/(2\chi)$ for their ratio $R = \beta/\alpha$.

Numerical simulations.—Let us compare our analytical findings with numerical simulations. Numerical approaches to the Sauter-Schwinger effect include direct integrations of the Klein-Fock-Gordon or Dirac equations (see, e.g., [58–63]), a reformulation in terms of the Heisenberg-Wigner formalism (see, e.g., [64–67]), quantum Monte Carlo methods (see, e.g., [68]), or numerical world-line instanton solvers (see, e.g., [69,70]). Each of these methods has advantages and drawbacks, but calculating an exponentially small pair-creation probability P in a complex higher-dimensional field configuration $\boldsymbol{A}(t,\boldsymbol{r})$ is always challenging.

In order to reduce the computational complexity as much as possible, we consider the Dirac equation in $2+1$ dimensions, where we can use two-component spinors, but still incorporate a transversal field (2). Employing the Dirac-Heisenberg-Wigner formalism, the problem is mapped onto a set of first-order transport equations involving bilinear expectation values, see Sec. B in Supplemental Material [35].

We consider the following field profile in Eq. (2)

$$f(t) = \frac{Et}{2}\exp\{-\omega^2 t^2\}, \tag{16}$$

which displays the maximum electric field E at $t = 0$ and $x = 0$. Since the vector potential vanishes asymptotically $f(t \to \pm\infty) = 0$ the wave number k_y coincides with the mechanical momentum at those times. This simplifies the numerical analysis and will be relevant for the pair-creation spectra discussed in Sec. D in Supplemental Material [35].

Numerical results.—In the following, we set the field parameter E in Eq. (16) to $E = E_S/3$, i.e., the peak field strength is one third of the Schwinger critical field. In this case, we are already in the subcritical regime where the pair-creation probability P is exponentially suppressed as in Eq. (1), but the numbers are not too small for a reliable numerical computation.

The computed mean particle numbers are plotted in Fig. 1. The locally constant field approximation just reflects the trivial space-time volume scaling with $1/\omega^2$.

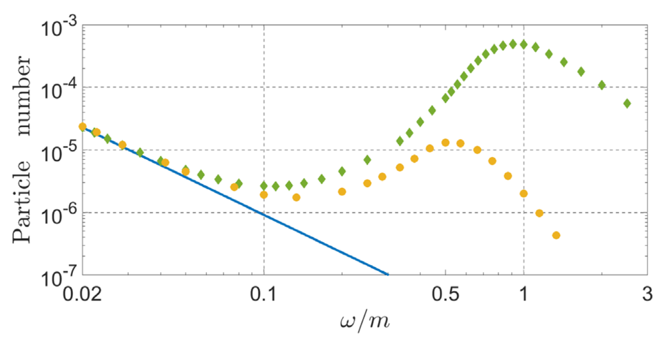

FIG. 1. Plot of the mean number of created particles as a function of ω for the profile (16) with $E = E_S/3$. The yellow circles denote the results of the Dirac-Heisenberg-Wigner formalism, the green diamonds correspond to the spatially homogeneous field approximation and the blue line displays the locally constant field approximation.

As expected, the results of the Dirac-Heisenberg-Wigner formalism converge to that approximation for small ω, i.e., small Keldysh parameters (3), but start to show significant deviations for Keldysh parameters of order unity, which is the regime we are interested in.

Motivated by the above findings based on the WKB approach, we also compared those results with the spatially homogeneous field approximation: to this end, we calculated the pair-creation probability P for a purely time-dependent scenario $\boldsymbol{A}(t) = 2f(ct)\boldsymbol{e}_y$ corresponding to the field at the symmetry plane $x = 0$ [71–73]. While this is expected to yield the correct pair-creation exponent, this scenario grossly overestimates the prefactor because particles are now created in the whole spatial volume. For the colliding pulses (2), however, pair creation predominantly occurs in the vicinity of the symmetry plane $x = 0$ where the electric field assumes its maximum. In order to correct this overestimation, we introduce a prefactor accounting for the finite extent (in the x direction) of the effective pair-creation volume [74]. As a natural and minimal assumption, we take this prefactor to be proportional to $1/\omega$, i.e., the pulse width, where the proportionality constant is fixed by demanding convergence to the locally constant field approximation at small ω, see also Refs. [76–80].

As we may observe in Fig. 1, this spatially homogeneous field approximation still overestimates the pair-creation probability a bit, but provides a much better description than the locally constant field approximation. Even for frequencies of the order of the electron mass, it reproduces the qualitative behavior of the full Dirac-Heisenberg-Wigner results, such as the peak of the particle number at $\omega = \mathcal{O}(m)$. The quantitative disagreement regarding the height and location of the peaks can presumably be explained by a threshold effect marking the transition from the nonperturbative (Sauter-Schwinger) to the perturbative (Breit-Wheeler [81]) regime at large ω (where the WKB approach is expected to break down), see Sec. E in Supplemental Material [35].

Focusing and defocusing corrections.—The spatially homogeneous field approximation explained above does only take into account the $\ddot{s}$ term in Eqs. (15), i.e., the electric field E_y. In order to include the effects of the magnetic field B_z, one should replace $\ddot{s} \to \Box s$, cf. Eqs. (15), which also contains $\partial_x^2 s$, i.e., the curvature s_2 in Eq. (10). The effect of this replacement can be studied by numerically solving the set of ordinary differential equations (8), (10), and (15) for the profile (16). As example parameters, we choose $E = E_S/3$ as before and $\omega = m/3$, i.e., $\gamma = 1$.

As shown in Sec. C of Supplemental Material [35], the behavior of $\ddot{s}_0(t)$ and $s_2(t)$ strongly depends on the momentum k_y. For $k_y = \pm m$, for example, the curvature $s_2(t)$ is quite close to $\ddot{s}_0(t)$ thus almost canceling each other in the prefactor $\Box s$. For $k_y = 0$, this is not the case as the curvature $s_2(t)$ varies more slowly with time than $\ddot{s}_0(t)$.

We find that including the curvature term s_2 reduces the pair-creation probability, e.g., roughly by a factor of 2 for the case $k_y = 0$ (which yields the dominant contribution), see Sec. C in Supplemental Material [35]. Thus, including the focusing and defocusing effects corrects the overestimate of the spatially homogeneous field approximation and brings the estimated pair-creation probability almost on top of the value obtained by the Dirac-Heisenberg-Wigner approach, see Sec. I in Supplemental Material [35]. However, more systematic investigations are needed to assess the overall accuracy of this approach.

Conclusions.—As a prototypical example for a space-time dependent and transversal field configuration (as a vacuum solution to the Maxwell equations), we consider the head-on collision of two plane-wave laser pulses. Via the WKB approach, we study electron-positron pair creation in this background for subcritical fields $E \ll E_S$ and Keldysh parameters of order unity. Along the symmetry (i.e., collision) plane, where we expect that dominant contribution, we find that the pair-creation exponent is the same as for a purely time-dependent electric field, only the prefactor $\ddot{s} \to \Box s$ does also include the impact of the magnetic field, leading to focusing and defocusing effects.

This approximate mapping to a purely time-dependent electric field allows us to employ the spatially homogeneous field approximation, which we compare to numerical simulations using the Dirac-Heisenberg-Wigner approach. We find that the spatially homogeneous field approximation overestimates the pair-creation probability slightly, but provides a much better description than the locally constant field approximation, see Fig. 1. It even reproduces qualitative features of the pair-creation spectra, see Sec. D in Supplemental Material [35].

Going beyond the spatially homogeneous field approximation, we may also study the impact of the magnetic field, leading to focusing and defocusing effects. Along the symmetry plane, this amounts to replacing $\ddot{s}$ by $\Box s$ in the evolution equations for the Bogoliubov coefficients, which also contains the curvature term $\partial_x^2 s$. For the cases we studied, we found that this replacement tends to lower the pair-creation probability, which brings it closer to the results of the Dirac-Heisenberg-Wigner approach, see Secs. C and I in Supplemental Material [35].

However, one might also imagine other scenarios. Note that $\ddot{s}$ is a local function of A_y and $\dot{A}_y$, while the curvature $\partial_x^2 s$ is nonlocal, i.e., depends on whole history of the evolution. This could be exploited in pulse-shape optimization schemes aimed at increasing the pair-creation probability. As an intuitive picture, if the initial wave packet of the fermionic quantum vacuum fluctuations is focused onto the symmetry plane, where the electric field assumes its maximum, it can react to this strong field (i.e., produce particles) much better than a wave packet which is more delocalized. In summary, our findings motivate further studies of this phenomenon.

Experimental scenarios.—Finally, let us discuss potential experimental tests of our results [83,84]. Ultrastrong optical laser foci have very small Keldysh parameters $\gamma \ll 1$ and should thus be treatable via the locally constant field approximation. X-ray free electron lasers, on the other hand, have much larger γ and could require going beyond that approximation. Unfortunately, however, present-day facilities do not reach the necessary field strengths E yet [82]. An interesting idea to achieve this goal is high-harmonic focusing (see, e.g., [85–87]) which typically also corresponds to non-negligible γ.

As a completely different scenario for generating ultrastrong fields, collisions of heavy nuclei have been studied theoretically and experimentally, see, e.g., [88–93]. Considering ultraperipheral "collisions" at relativistic velocities v along the trajectories $\boldsymbol{r}(t) = \pm(vt, b/2, 0)^T$ with impact parameters b, the superpositions of the boosted Coulomb fields of the two nuclei can be approximated by Eq. (2) at sufficiently large distances $|\boldsymbol{r}| \gg b$, say, of the order of the Compton length [94,96]. The associated field strengths may reach or even exceed the Schwinger critical field E_S [99,100] and the Keldysh parameters γ will also be non-negligible (especially for ultrarelativistic v). Of course, the field strengths and their spatial and temporal gradients will be even larger at smaller distances $|\boldsymbol{r}| \sim b$, such that the total electron-positron yield will also contain contributions from this region. Nevertheless, this again shows the importance of understanding the impact of space-time dependence on pair creation, i.e., to go beyond the locally constant field approximation.

We thank Christian Schneider and Christian Schubert for fruitful discussions. R. S. acknowledges support by the Deutsche Forschungsgemeinschaft (DFG, German Research Foundation)–Project-ID 278162697–SFB 1242.

[1] W. Heisenberg and H. Euler, Consequences of Dirac's theory of positrons, Z. Phys. **98**, 714 (1936).

[2] V. Weisskopf, Über die Elektrodynamik des Vakuums auf Grund der Quantentheorie des Elektrons, Kong. Dan. Vid. Sel. Mat. Fys. Med. **14N6**, 1 (1936).

[3] J. S. Schwinger, On gauge invariance and vacuum polarization, Phys. Rev. **82**, 664 (1951).

[4] F. Sauter, Über das Verhalten eines Elektrons im homogenen elektrischen Feld nach der relativistischen Theorie Diracs, Z. Phys. **69**, 742 (1931).

[5] T. Heinzl, B. King, and A. J. MacLeod, Locally monochromatic approximation to QED in intense laser fields, Phys. Rev. A **102**, 063110 (2020).

[6] D. Seipt and B. King, Spin- and polarization-dependent locally-constant-field-approximation rates for nonlinear Compton and Breit-Wheeler processes, Phys. Rev. A **102**, 052805 (2020).

[7] A. I. Nikishov and V. I. Ritus, Quantum processes in the field of a plane electromagnetic wave and in a constant field I, Sov. Phys. JETP **19**, 529 (1964); J. Exp. Theor. Phys. **46**, 776 (1964).

[8] S. P. Kim and D. N. Page, Schwinger pair production in electric and magnetic fields, Phys. Rev. D **73**, 065020 (2006).

[9] R. Schützhold, H. Gies, and G. Dunne, Dynamically Assisted Schwinger Mechanism, Phys. Rev. Lett. **101**, 130404 (2008).

[10] G. V. Dunne, H. Gies, and R. Schützhold, Catalysis of Schwinger vacuum pair production, Phys. Rev. D **80**, 111301(R) (2009).

[11] A. Otto, D. Seipt, D. Blaschke, B. Kämpfer, and S. A. Smolyansky, Lifting shell structures in the dynamically assisted Schwinger effect in periodic fields, Phys. Lett. B **740**, 335 (2015).

[12] S. Villalba-Chávez and C. Müller, Signatures of the Schwinger mechanism assisted by a fast-oscillating electric field, Phys. Rev. D **100**, 116018 (2019).

[13] For example, HIBEF, LUXE, ELI, CILEX, CoReLS, ShenGuang-II as well as SLAC; cf. the websites https://www.hibef.eu/, https://luxe.desy.de/, https://www.eli-beams.eu/, https://eli-laser.eu/, https://cilexsaclay.fr/, https://corels.ibs.re.kr/, https://lssf.cas.cn/en/, https://www6.slac.stanford.edu/.

[14] A. R. Bell and J. G. Kirk, Possibility of Prolific Pair Production with High-Power Lasers, Phys. Rev. Lett. **101**, 200403 (2008).

[15] S. S. Bulanov, T. Zh. Esirkepov, A. G. R. Thomas, J. K. Koga, and S. V. Bulanov, Schwinger Limit Attainability with Extreme Power Lasers, Phys. Rev. Lett. **105**, 220407 (2010).

[16] S. P. Kim and D. N. Page, Improved approximations for fermion pair production in inhomogeneous electric fields, Phys. Rev. D **75**, 045013 (2007).

[17] H. Kleinert, R. Ruffini, and S.-S. Xue, Electron-positron pair production in space- or time-dependent electric fields, Phys. Rev. D **78**, 025011 (2008).

[18] T. Heinzl, A. Ilderton, and M. Marklund, Finite size effects in stimulated laser pair production, Phys. Lett. B **692**, 250 (2010).

[19] F. Hebenstreit, A. Ilderton, and M. Marklund, Pair production: The view from the lightfront, Phys. Rev. D **84**, 125022 (2011).

[20] G. V. Dunne and C. Schubert, Worldline instantons and pair production in inhomogenous fields, Phys. Rev. D **72**, 105004 (2005).

[21] A. Di Piazza, M. Tamburini, S. Meuren, and C. M. Keitel, Improved local-constant-field approximation for strong-field QED codes, Phys. Rev. A **99**, 022125 (2019).

[22] I. A. Aleksandrov, G. Plunien, and V. M. Shabaev, Momentum distribution of particles created in space-time-dependent colliding laser pulses, Phys. Rev. D **96**, 076006 (2017).

[23] A. Ilderton, Exact results for scattering on ultrashort plane wave backgrounds, Phys. Rev. D **100**, 125018 (2019).

[24] A. M. Fedotov and A. A. Mironov, Pair creation by collision of intense laser pulse with high-frequency photon beam, Phys. Rev. A **88**, 062110 (2013).

[25] G. Torgrimsson, C. Schneider, and R. Schützhold, Sauter-Schwinger pair creation dynamically assisted by a plane wave, Phys. Rev. D **97**, 096004 (2018).

[26] C. Banerjee, M. P. Singh, and A. M. Fedotov, Phase control of Schwinger pair production by colliding laser pulses, Phys. Rev. A **98**, 032121 (2018).

[27] H. R. Reiss, Absorption of light by light, J. Math. Phys. (N.Y.) **3**, 59 (1962).

[28] L. V. Keldysh, Ionization in the field of a strong electromagnetic wave, Sov. Phys. JETP **20**, 1307 (1965); J. Exp. Theor. Phys. **47**, 1945 (1964).

[29] A. M. Perelomov, V. S. Popov, and M. V. Terent'ev, Ionization of atoms in an alternating electric field, I and II, Sov. Phys. JETP **23**, 924 (1966); **24**, 207 (1967); J. Exp. Theor. Phys. **50**, 1393 (1966); **51**, 309 (1966).

[30] V. S. Popov, Tunnel and multiphoton ionization of atoms and ions in a strong laser field (Keldysh theory), Phys. At. Nucl. **68**, 686 (2005).

[31] A. Fedotov, A. Ilderton, F. Karbstein, B. King, D. Seipt, H. Taya, and G. Torgrimsson, Advances in QED with intense background fields, arXiv:2203.00019.

[32] I. K. Affleck, O. Alvarez, and N. S. Manton, Pair production at strong coupling in weak external fields, Nucl. Phys. **B197**, 509 (1982).

[33] M. F. Linder, C. Schneider, J. Sicking, N. Szpak, and R. Schützhold, Pulse shape dependence in the dynamically assisted Sauter-Schwinger effect, Phys. Rev. D **92**, 085009 (2015).

[34] C. K. Dumlu and G. V. Dunne, Complex worldline instantons and quantum interference in vacuum pair production, Phys. Rev. D **84**, 125023 (2011).

[35] See Supplemental Material at http://link.aps.org/supplemental/10.1103/PhysRevLett.129.241801, which includes Refs. [36–50], for more details.

[36] G. V. Dunne, Q.-h. Wang, H. Gies, and C. Schubert, Worldline instantons and the fluctuation prefactor, Phys. Rev. D **73**, 065028 (2006).

[37] D. Vasak, M. Gyulassy, and H. T. Elze, Quantum transport theory for Abelian plasmas, Ann. Phys. (N.Y.) **173**, 462 (1987).

[38] G. Fauth, J. Berges, and A. Di Piazza, Collisional strong-field QED kinetic equations from first principles, Phys. Rev. D **104**, 036007 (2021).

[39] J. C. R. Bloch, V. A. Mizerny, A. V. Prozorkevich, C. D. Roberts, S. M. Schmidt, S. A. Smolyansky, and D. V. Vinnik, Pair creation: Back reactions and damping, Phys. Rev. D **60**, 116011 (1999).

[40] F. Gelis and N. Tanji, Formulation of the Schwinger mechanism in classical statistical field theory, Phys. Rev. D **87**, 125035 (2013).

[41] A. M. Fedotov, N. B. Narozhny, G. Mourou, and G. Korn, Limitations on the Attainable Intensity of High Power Lasers, Phys. Rev. Lett. **105**, 080402 (2010); **105**, 199901 (E) (2010).

[42] N. V. Elkina, A. M. Fedotov, I. Yu. Kostyukov, M. V. Legkov, N. B. Narozhny, E. N. Nerush, and H. Ruhl, QED cascades induced by circularly polarized laser fields, Phys. Rev. ST Accel. Beams **14**, 054401 (2011).

[43] I. Bialynicki-Birula, P. Górnicki, and J. Rafelski, Phase-space structure of the Dirac vacuum, Phys. Rev. D **44**, 1825 (1991).

[44] S. Ochs and U. Heinz, Wigner functions in covariant and single-time formulations, Ann. Phys. (N.Y.) **266**, 351 (1998).

[45] C. Kohlfürst and R. Alkofer, On the effect of time-dependent inhomogeneous magnetic fields in electron-positron pair production, Phys. Lett. B **756**, 371 (2016).

[46] C. Kohlfürst, The Heisenberg-Wigner formalism for transverse fields (to be published).

[47] A. I. Nikishov, Pair production by a constant external field, Sov. Phys. JETP **30**, 660 (1970); J. Exp. Theor. Phys. **57**, 1210 (1969).

[48] Q. Lin, Electron-positron pair creation in a vacuum by an electromagnetic field in $3 + 1$ and lower dimensions, J. Phys. G **25**, 17 (1999).

[49] E. Akkermans and G. V. Dunne, Ramsey Fringes and Time-Domain Multiple-Slit Interference from Vacuum, Phys. Rev. Lett. **108**, 030401 (2012).

[50] J. Z. Kamiński, M. Twardy, and K. Krajewska, Diffraction at a time grating in electron-positron pair creation from the vacuum, Phys. Rev. D **98**, 056009 (2018).

[51] A. Di Piazza, Ultrarelativistic Electron States in a General Background Electromagnetic Field, Phys. Rev. Lett. **113**, 040402 (2014).

[52] H. Taya, T. Fujimori, T. Misumi, M. Nitta, and N. Sakai, Exact WKB analysis of the vacuum pair production by time-dependent electric fields, J. High Energy Phys. 03 (2021) 082.

[53] V. P. Maslov and M. V. Fedoriuk, *Semi-Classical Approximation in Quantum Mechanics* (Springer Science & Business Media, New York, 2001).

[54] This expectation is confirmed by our numerical results, see Supplemental Material [35], as long as no large frequency scales $\omega = \mathcal{O}(m)$ are considered, where we enter the perturbative regime and threshold effects start to play a role.

[55] J. Oertel and R. Schützhold, WKB approach to pair creation in spacetime-dependent fields, Phys. Rev. D **99**, 125014 (2019).

[56] C. K. Dumlu and G. V. Dunne, Interference effects in Schwinger vacuum pair production for time-dependent laser pulses, Phys. Rev. D **83**, 065028 (2011).

[57] V. S. Popov, Pair production in a variable and homogeneous electric field as an oscillator problem, Sov. Phys. JETP **35**, 659 (1972); J. Exp. Theor. Phys. **62**, 1248 (1972).

[58] I. A. Aleksandrov, G. Plunien, and V. M. Shabaev, Electron-positron pair production in external electric fields varying both in space and time, Phys. Rev. D **94**, 065024 (2016).

[59] M. Ruf, G. R. Mocken, C. Müller, K. Z. Hatsagortsyan, and C. H. Keitel, Pair Production in Laser Fields Oscillating in Space and Time, Phys. Rev. Lett. **102**, 080402 (2009).

[60] Q. Z. Lv, S. Dong, Y. T. Li, Z. M. Sheng, Q. Su, and R. Grobe, Role of the spatial inhomogeneity on the laser-induced vacuum decay, Phys. Rev. A **97**, 022515 (2018).

[61] G. R. Mocken, M. Ruf, C. Müller, and C. H. Keitel, Nonperturbative multiphoton electron-positron–pair creation in laser fields, Phys. Rev. A **81**, 022122 (2010).

[62] Z.-L. Li, D. Lu, and B.-S. Xie, Multiple-slit interference effect in the time domain for boson pair production, Phys. Rev. D **89**, 067701 (2014).

[63] Q. Z. Lv, A. C. Su, M. Jiang, Y. J. Li, R. Grobe, and Q. Su, Pair creation for bosons in electric and magnetic fields, Phys. Rev. A **87**, 023416 (2013).

[64] C. Kohlfürst, On the effect of time-dependent inhomogeneous magnetic fields on the particle momentum spectrum in electron-positron pair production, Phys. Rev. D **101**, 096003 (2020).

[65] I. A. Aleksandrov and C. Kohlfürst, Pair production in temporally and spatially oscillating fields, Phys. Rev. D **101**, 096009 (2020).

[66] F. Hebenstreit, J. Berges, and D. Gelfand, Simulating fermion production in 1+1 dimensional QED, Phys. Rev. D **87**, 105006 (2013).

[67] H. Al-Naseri, J. Zamanian, and G. Brodin, Plasma dynamics and vacuum pair creation using the Dirac-Heisenberg-Wigner formalism, Phys. Rev. E **104**, 015207 (2021).

[68] H. Gies and K. Klingmuller, Pair production in inhomogeneous fields, Phys. Rev. D **72**, 065001 (2005).

[69] C. Schneider and R. Schützhold, Dynamically assisted Sauter-Schwinger effect in inhomogeneous electric fields, J. High Energy Phys. 02 (2016) 164.

[70] C. Schneider, G. Torgrimsson, and R. Schützhold, Discrete worldline instantons, Phys. Rev. D **98**, 085009 (2018).

[71] F. Hebenstreit, R. Alkofer, and H. Gies, Schwinger pair production in space- and time-dependent electric fields: Relating the Wigner formalism to quantum kinetic theory, Phys. Rev. D **82**, 105026 (2010).

[72] Y. Kluger, J. M. Eisenberg, B. Svetitsky, F. Cooper, and E. Mottola, Fermion pair production in a strong electric field, Phys. Rev. D **45**, 4659 (1992).

[73] S. M. Schmidt, D. B. Blaschke, G. Röpke, S. A. Smolyansky, A. V. Prozorkevich, and V. D. Toneev, A quantum kinetic equation for particle production in the Schwinger mechanism, Int. J. Mod. Phys. E **07**, 709 (1998).

[74] Note that the spatially homogeneous field approximation applied here is not synonymous with the locally homogeneous approximation used in, for example, [75]. In the latter, the field $A(t,x)$ at each space point x is mapped onto a purely time-dependent field and the resulting pair creation density is then integrated over all positions x (in analogy to the locally constant field approximation, just with x instead of x and t). Thus, this approximation scheme completely neglects the impact of the magnetic field component [64]. As a result, it would yield a finite particle creation rate even for a single propagating pulse $\boldsymbol{A}(t,\boldsymbol{r}) = A_y(t,x)\boldsymbol{e}_y = f(t-x)\boldsymbol{e}_y$ which is not correct.

[75] F. Hebenstreit, R. Alkofer, and H. Gies, Particle Self-Bunching in the Schwinger Effect in Spacetime-Dependent Electric Fields, Phys. Rev. Lett. **107**, 180403 (2011).

[76] A. Blinne and E. Strobel, Comparison of semiclassical and Wigner function methods in pair production in rotating fields, Phys. Rev. D **93**, 025014 (2016).

[77] E. Strobel and S.-S. Xue, Semiclassical pair production rate for rotating electric fields, Phys. Rev. D **91**, 045016 (2015).

[78] E. Strobel and S.-S. Xue, Semiclassical pair production rate for time-dependent electrical fields with more than one component: WKB-approach and world-line instantons, Nucl. Phys. **B886**, 1153 (2014).

[79] I. A. Aleksandrov, G. Plunien, and V. M. Shabaev, Locally-constant field approximation in studies of electron-positron pair production in strong external fields, Phys. Rev. D **99**, 016020 (2019).

[80] F. Hebenstreit, R. Alkofer, and H. Gies, Pair production beyond the Schwinger formula in time-dependent electric fields, Phys. Rev. D **78**, 061701(R) (2008).

[81] G. Breit and J. A. Wheeler, Collision of two light quanta, Phys. Rev. **46**, 1087 (1934).

[82] A. Ringwald, Pair production from vacuum at the focus of an x-ray free electron laser, Phys. Lett. B **510**, 107 (2001).

[83] X. Ribeyre, E. d'Humiéres, O. Jansen, S. Jequier, V. T. Tikhonchuk, and M. Lobet, Pair creation in collision of γ-ray beams produced with high-intensity lasers, Phys. Rev. E **93**, 013201 (2016).

[84] J. Q. Yu, H. Y. Lu, T. Takahashi, R. H. Hu, Z. Gong, W. J. Ma, Y. S. Huang, C. E. Chen, and X. Q. Yan, Creation of Electron-Positron Pairs in Photon-Photon Collisions Driven by 10-PW Laser Pulses, Phys. Rev. Lett. **122**, 014802 (2019).

[85] S. Gordienko, A. Pukhov, O. Shorokhov, and T. Baeva, Coherent Focusing of High Harmonics: A New Way Towards the Extreme Intensities, Phys. Rev. Lett. **94**, 103903 (2005).

[86] H. Vincenti, Achieving Extreme Light Intensities Using Optically Curved Relativistic Plasma Mirrors, Phys. Rev. Lett. **123**, 105001 (2019).

[87] L. Fedeli, A. Sainte-Marie, N. Zaim, M. Thévenet, J. L. Vay, A. Myers, F. Quéré, and H. Vincenti, Probing Strong-Field QED with Doppler-Boosted Petawatt-Class Lasers, Phys. Rev. Lett. **127**, 114801 (2021).

[88] J. Adam *et al.* (STAR Collaboration), Measurement of e^+e^- Momentum and Angular Distributions from Linearly Polarized Photon Collisions, Phys. Rev. Lett. **127**, 052302 (2021).

[89] J. Reinhardt, B. Müller, and W. Greiner, Theory of positron production in heavy-ion collisions, Phys. Rev. A **24**, 103 (1981).

[90] J. Schweppe, A. Gruppe, K. Bethge, H. Bokemeyer, T. Cowan, H. Folger, J. S. Greenberg, H. Grein, S. Ito, R. Schule, D. Schwalm, K. E. Stiebing, N. Trautmann, P. Vincent, and M. Waldschmidt, Observation of a Peak Structure in Positron Spectra from U + Cm Collisions, Phys. Rev. Lett. **51**, 2261 (1983).

[91] T. Cowan, H. Backe, K. Bethge, H. Bokemeyer, H. Folger, J. S. Greenberg, K. Sakaguchi, D. Schwalm, J. Schweppe, K. E. Stiebing, and P. Vincent, Observation of Correlated Narrow-Peak Structures in Positron and Electron Spectra from Superheavy Collision Systems, Phys. Rev. Lett. **56**, 444 (1986).

[92] I. Ahmad *et al.* (APEX Collaboration), Search for Monoenergetic Positron Emission from Heavy-Ion Collisions at Coulomb-Barrier Energies, Phys. Rev. Lett. **78**, 618 (1997).

[93] I. A. Maltsev, V. M. Shabaev, R. V. Popov, Y. S. Kozhedub, G. Plunien, X. Ma, T. Stöhlker, and D. A. Tumakov,

How to Observe the Vacuum Decay in Low-Energy Heavy-Ion Collisions, Phys. Rev. Lett. **123**, 113401 (2019).

[94] On a different length scale, one could also consider tightly focused electron bunches instead of the nuclei, see also Ref. [95].

[95] V. Yakimenko, S. Meuren, F. Del Gaudio, C. Baumann, A. Fedotov, F. Fiuza, T. Grismayer, M. J. Hogan, A. Pukhov, L. O. Silva, and G. White, Prospect of Studying Nonperturbative QED with Beam-Beam Collisions, Phys. Rev. Lett. **122**, 190404 (2019).

[96] For the Schwinger production of magnetic monopoles, see Refs. [97,98].

[97] O. Gould, D. L.-J. Ho, and A. Rajantie, Schwinger pair production of magnetic monopoles: Momentum distribution for heavy-ion collisions, Phys. Rev. D **104**, 015033 (2021).

[98] O. Gould, D. L.-J. Ho, and A. Rajantie, Towards Schwinger production of magnetic monopoles in heavy-ion collisions, Phys. Rev. D **100**, 015041 (2019).

[99] M. Y. Şengül, M. C. Güçlü, Ö. Mercan, and N. G. Karakuş, Electromagnetic heavy-lepton pair production in relativistic heavy-ion collisions, Eur. Phys. J. C **76**, 428 (2016).

[100] ATLAS Collaboration, Evidence for light-by-light scattering in heavy-ion collisions with the ATLAS detector at the LHC, Nat. Phys. **13**, 852 (2017).